DWCNT-Doped Silica Gel Exhibiting Both Ionic and Electronic Conductivities

Benjamin Le Ouay, Stephanie Lau-Truong, Emmanuel Flahaut, Roberta Brayner, Jean Aubard, Thibaud Coradin, Christel Laberty-Robert

DWCNT-Doped Silica Gel Exhibiting Both Ionic and Electronic Conductivities

Benjamin Le Ouay,[†] Stéphanie Lau-Truong,[‡] Emmanuel Flahaut,[§] Roberta Brayner,[‡] Jean Aubard,[‡] Thibaud Coradin,[†] and Christel Laberty-Robert*[,†]

[†]Laboratoire de Chimie de la Matière Condensée de Paris (LCMCP), CNRS-UMR 7574, Université Pierre et Marie Curie Paris-6, Collège de France, 11 place Marcelin Berthelot, F-75005 Paris, France

[‡]ITODYS, Université Denis Diderot Paris-7, 15 rue Jean Antoine de Baïf, F-75013 Paris, France

[§]CIRIMAT-LCMIE, UMR 5085, Université Paul Sabatier Toulouse-3, 118 route de Narbonne, F-31062 Toulouse, France

ABSTRACT: Silica gels doped with double-walled carbon nanotubes (DWCNTs) were prepared using an aqueous sol–gel route in mild conditions (neutral pH, room temperature). The wet gels exhibited both ionic and electronic conduction. Electrochemical impedance spectroscopy was used to study these two different conduction pathways that prevail at different characteristic time scales. The ionic conduction in the silica network was found to be independent of the DWCNT-doping rate. The electronic conduction through the DWCNT network was found to occur above a critical concentration (0.175 wt %) corresponding to nanotube percolation threshold. The highest content in DWCNTs (0.8 wt %) exhibited a conductivity of 0.05 S/m. Furthermore, the DWCNTs network was found to evolve even after the macroscopic solidification of the gel, suggesting a reorganization of the DWCNTs at the molecular level. This phenomenon could be attributed to the polarization effect of the electrode and was confirmed by Raman spectroscopy studies. Such materials can be useful for the design of sensors incorporating electroactive chemical or biological species.

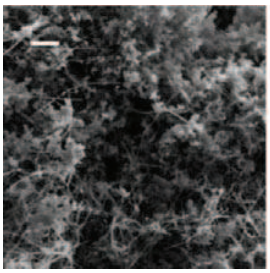

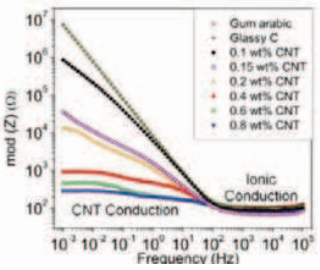

1. INTRODUCTION

Carbon nanotubes (CNTs) possess remarkable physical and chemical properties[1−3] such as excellent tensile strength,[4] high thermal[5] and electrical conductivity, and unique electronic properties.[6] They have therefore been considered as useful nanomaterials for a wide range of application[7,8] such as composite materials,[9] scanning probe microscopy,[10] sensor development,[11] energy storage,[12] nanoelectronics,[13] and field emission.[14] In particular, their electrical conductivity together with their very high aspect ratio (>1000) makes them suitable for use as conductive fillers dispersed in insulating matrices.[15] Such nanocomposites can exhibit a significant conductivity provided that the loading in conductive CNTs is high enough to allow the formation of a percolative network. Thanks to their very high anisotropy, the percolation threshold can be reached at concentrations that are several orders of magnitude lower than what can be obtained with spherical particles, such as carbon black.[16] The incorporation of a small proportion of CNTs in such matrices gives them an electrical conductivity of ca. 1 S/cm for highly doped (>2 wt %) materials, without significantly hindering too much, and sometimes even improving, the other properties of the matrix.[16−18]

Several materials have been evaluated as a host matrix for the CNTs network. Most of the research has been focused on their encapsulation in polymer,[16,19,20] ceramics,[18,21,22] or sol–gel-based matrices.[23−25] The latter technology has the advantage of being performed in mild conditions that not only limit the possible degradation of the nanotubes but also allow the incorporation of bio-organic molecules in the materials, opening the route to the design of specific electrochemical sensors.[26,27] However, wet sol–gel materials evolve upon aging. Ostwald ripening, a succession of local reactions of dissolution and reprecipitation, modifies the microstructure of the gel over time.[28] It is also important to consider that the inorganic network is highly porous, with only a few percents of the volume occupied by the solid phase necessary to get a self-standing material. This leaves a great fraction of the volume filled by liquid, in which some mobility and structural reorganization can occur. Although the dynamic reorganization of CNTs have already been studied in liquid media, demonstrating the progressive formation of a percolative network, together with an alignment of the nanotubes,[29] this aspect, to our knowledge, has been only scarcely studied within composites materials. This is due to the fact that the host

matrices were either very dense[24] or because the materials were dried and solidified before characterization.[25]

The present work focused on the preparation and characterization of the conduction properties of silica gels doped with CNTs. Double-walled carbon nanotubes (DWCNTS) were selected as optimal carbon form to obtain high conductivity at minimal loading since they combine the respective advantages of single-walled and multiwalled CNTs, i.e., a low mass per unit of length, a higher proportion of conductive CNTs, and the presence of a protective outer wall. The procedure for silica gel formation was developed foreseeing future development of sensor devices. Therefore, an aqueous route performed at neutral pH and room temperature was selected. Gum arabic, a biopolymer that possess a great affinity toward carbon materials,[30] was chosen over the more commonly used SDS (sodium dodecyl sulfonate) and SDBS (sodium dodecyl benzylsulfonate) to disperse the DWCNTs. This polymer was chosen because of its limited detergent effect and its lack of cytotoxicity.[31] The procedure was also adapted so that a significant amount (22 vol % of the final gel) of water is added once the sol is neutralized and the DWCNTs dispersed, but prior to the gelation. In order to give the gels functional properties, this water could be substituted by an aqueous solution containing fragile species or chemical assemblies.

Impedance spectroscopy was used to characterize the materials, and a model was proposed to explain their conductive behavior. We show that the presence of significant quantities of water in the materials allowed diffusion or migration of solvated species. Our model allows discriminating electric conduction from ionic one. Additionally, these two processes can be assessed quantitatively. Raman spectroscopy was used to characterize the CNTs population present in the samples. It provides information both on the individual electronic structure of the tubes, through the position and intensity of some specific peaks, and on the aggregation state of the CNTs, through peak broadening while the nanotubes form bundles. We demonstrate here, for the first time to our knowledge, that such reorganization occurs within the silica gel due to the polarization applied within the electrochemical cells. Such reorganization decreases the electrical resistance of the material and should be taken into account for the future design of electrochemical sensors based on organic or biological encapsulation within these silica−CNT nanocomposites.

2. EXPERIMENTAL SECTION

Preparation of the Gels. Double-wall carbon nanotubes (DWCNTs) were prepared by catalytic chemical vapor deposition (CCVD) using a Co:Mo−MgO catalyst, following a methodology developed by Flahaut et al.[32] Briefly after the CCVD synthesis, the DWCNTs were washed with a solution of concentrated HCl in order to dissolve the catalyst without functionalizing the nanotubes. The DWCNTs were washed with deionized water until neutral pH is reached and dried. A sol was prepared by mixing the required amount of DWCNTs with 1.5 g of an aqueous solution (5 wt %) of gum arabic (Acacia tree, Sigma), 1.0 g of a sodium silicate solution (0.66 mol L^{-1}, Riedel-de-Haen), and 1.3 g of LUDOX HS-40 (Sigma-Aldrich). The DWCNTs were dispersed using a ultrasound probe (MSE L665 (100W) and L667 probe) working at 80% of its nominal power for 30 min while cooled with an ice bath. Homogeneous suspension with no visible aggregate was obtained. This silica sol was then neutralized by the addition of 112 μL of hydrochloric acid (4 mol L^{-1}, VWR). Thirty seconds after neutralization, 1 mL of water was added to the sol. The gelation of the gel occurred in ca. 10 min, allowing the sol to be processed before it becomes a solid. Samples that contain 0.*XX* wt % DWCNTs are designated as CNT-*XX*. Furthermore, GA-0 and GC-80 contain respectively no carbonaceous charge and 0.8 wt % of glassy carbon (spherical particles, 2−12 μm, Aldrich).

Impedance Measurement. The measurement cell was constituted by a ring of PTFE (polytetrafluoroethylene) (thickness: 0.2 cm; inner surface: 4 cm^2) disposed between two indium−tin oxide (ITO)-coated glass slides (Solems, resistivity: 80 Ω/in.), maintained by binder clips. ITO electrodes were used since that material presents a certain inertia toward oxidation, and its transparency allows to perform optical spectroscopy experiments within the electrochemistry cell. Copper adhesive tape was used to provide a good connection between the ITO electrodes and the measurement apparatus. The silica sol was injected in the inner cavity with a syringe through one of two furrows carved in the PTFE ring. Grease and varnish were used to ensure a good tightness of the cell, and the furrows were sealed with wax in order to avoid the gel drying.

Impedance spectroscopy diagrams were recorded using a PAR 263A (EG&G Instruments) potensiostat coupled with a Solartron 1260 analyzer (Solartron Instruments). Diagrams were recorded between 100 kHz and 1 mHz (10 points/decade) with an amplitude of 25 mV.

FE-SEM Imaging. Scanning electron microscopy using a field emission gun (FE-SEM) was performed using a Zeiss Supra 40 apparatus operating at 20 kV. Prior to their observation, the water contained in the samples was exchanged with ethanol through a succession of water/ethanol baths (50, 70, 85, 95, and 100 vol %). Ethanol was then extracted with supercritical CO_2 using a LEICA EM CPD030 supercritical extractor.

Cryogenic Transmission Electron Microscopy. Grids with homemade holey carbon film were glow-discharged (EASY GLOW apparatus, PELCO) prior to sample deposition. Sample excess was removed by blotting with filter paper (Whatman #4) before plunging the grid in liquid ethane cooled by liquid nitrogen (homemade cryo-plunging device). Samples were analyzed by CryoTEM on Tecnai Spirit G2 FEI operating at 120 kV equipped with a Gatan cryo-holder 626DH operating at −180 °C. Images were recorded on a Gatan Orius 4K × 4K CCD camera.

Raman Spectroscopy. Raman spectra were obtained with a LABRAM HR 800 Jobin-Yvon microspectrometer. The microscope was equipped with a long working distance ×100 objective (NA: 0.60). The spectra have been recorded using 633 nm He−Ne laser excitation, and a XYmicrometer displacement stage was used to perform Raman mapping. Measurements were performed on several spots of the samples to ensure their homogeneities and to avoid degradation.

3. RESULTS AND DISCUSSION

The dispersion of the CNTs in the silica sol under sonication leads to a homogeneous suspension with no visible agglomerates. The duration of the sonication was chosen as the time where no aggregate was visible in the solution. A longer sonication time could have shortened the DWCNTs without improving their dispersion state and would have thus lowered their performances as electronic conductors. Since gum arabic is a biopolymer that contains hexoses and glucuronic

acid,[33] it is expected to be negatively charged in the silica sol both before (pH 10) and after its neutralization. Hence, the neutralization had no visible influence on the stability of the suspension. The synthesis leads to the formation of self-standing black monoliths of gel that are kept in closed reaction vessel in order to avoid drying. For the impedance measurements, the neutralized sol was introduced while it was still liquid and then formed a gel in the measurement cell (pictured in Figure 1), ensuring thus a good contact with the electrodes.

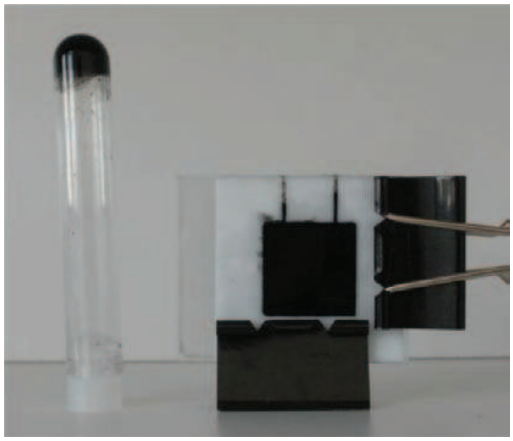

Figure 1. CNT-60 in a glass tube (upside down, left) and in a measurement cell (right).

Since no significant shrinkage occurred on the wet gel over a period of several weeks, the gel remained in contact with the electrodes during the whole period of measurement.

Effect of the Concentration of DWCNTs. Impedance spectrometry diagrams were recorded for samples containing between 0.1 and 0.8 wt % of DWCNTs. Another sample containing 0.8 wt % of glassy carbon (spherical particles, diameter: 12 μm) was synthesized to compare the effects of the morphology of the carbonaceous materials. Figure 2 shows the impedance diagrams (Bode representation) of those samples. These systems present three different regimes:

At very high frequency (between 100 and 30 kHz), every system possess an inductive behavior, with similar values of inductance. This behavior appears also while recording the impedance of a single ITO electrode. This phenomenon almost disappears when electrodes are constituted of a more conductive material (such as aluminum). This phenomenon can thus be attributed to the ITO electrode and/or to artifacts resulting from the equipment. However, because of the opacity of metals and the fact that most of the common metals are corroded in those conditions of salinity, ITO electrodes were used, even if they add supplementary phenomenon that must be taken into account.

At frequencies ranging from 30 kHz to 100 Hz, the effect of the inductive response becomes negligible, and the module of the impedance reaches a plateau. Moreover, the value of that plateau is similar for all the samples. This plateau has been attributed to the ionic conduction of both the Na^+ and Cl^- ions. These ions were introduced in the same quantities in all the samples with the gels precursors (mainly from the sodium silicate, LUDOX HS-40, and HCl for the neutralization and to a lesser extent other cations from the gum arabic).

At lower frequencies, between 100 Hz and 1 mHz, three responses domains can be distinguished, depending on the concentration in DWCNTs. In GA-0 and GC-80, which contain no CNTs, the modulus of the impedance is represented in the Bode plot by a line with a slope close to −1. The phase of the impedance reaches a plateau at −88°. This plateau is characteristic of a capacitive phenomenon that can be attributed to the accumulation of ions at the surface of the electrodes, compensating their polarization and blocking the current. The difference between the value of the phase and the one obtained for a perfect capacitor (−90°) is attributed to the roughness of the electrodes, leading to a slightly nonideal character of the electrodes. In CNTs-doped gels, two different behaviors appear depending on the concentration in CNTs. Under a threshold concentration, c_P, comprised between 0.1 and 0.2 wt %, the modulus of the impedance decreases with a slope close to −1 (in logarithmic plot) for intermediate frequencies. At lower frequencies, it decreases with different slope (absolute value is below 1). For gels that contain more CNTs than c_P (CNT-20 to CNT-80), the impedance modulus increases with the frequency decrease, until a plateau is reached at low frequency, and its phase reaches 0°. The height of that plateau decreases strongly with increasing c_{CNTs} for concentrations close to c_P.

Those two behaviors can be explained by the presence of a CNTs network encapsulated within the gel that percolates over a threshold concentration c_P comprised between 0.1 and 0.2 wt %. Over that concentration, the CNTs form a continuous network that allows the electrons to flow from an electrode to the other. Hence, a resistive component appears in gels that are sufficiently doped to allow the formation of that continuous network, and the phase of the impedance reaches 0° at low frequency. Unfortunately, this phenomena could occur only at very low frequencies (0.01 mHz and lower), which are

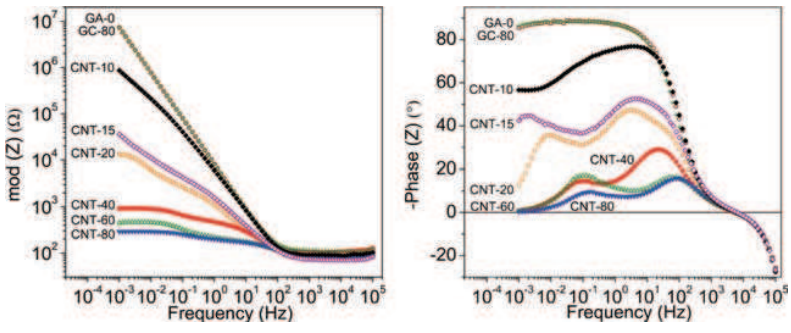

Figure 2. Bode plot (left: log |Z|; right: −Phase (Z)) of silica gels containing only gum arabic (GA-0), gum arabic and glassy carbon (GC-*XX*), or DWCNTs (CNT-*XX*). *XX* stands for the doping rate (0.*XX* wt %).

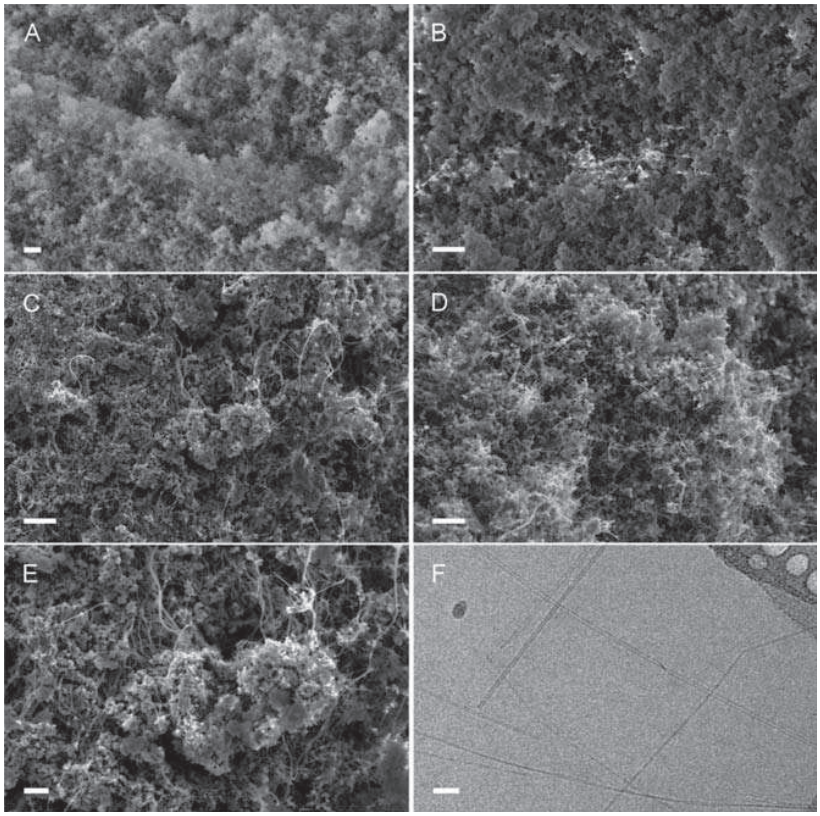

Figure 3. FE-SEM micrography of AG-0 (A), CNT-20 (B), CNT-60 (C, E), and CNT-80 (D) and cryo-TEM micrography (F) of the sol leading to CNT-60. The scale bar represents 500 nm in (A–D), 200 nm in (E), and 20 nm in (F).

impossible to reach experimentally, thus limiting the precision of the determination of c_p with this direct method.

The more CNTs a sample contains, the more connected the conductive network is. An increase in conductivity with the CNTs loading is observed. It is also noteworthy to mention that due to the very high aspect ratio of CNTs (L/d, where L is the length of the nanotube and d its diameter) and to their trend to associate themselves, the percolation fraction is very low. Note that this value would be much higher with spheres (L/d = 1, c_p about 30 vol %).[34] The capacitive behaviors that are present in the different gels find their origins in (i) the accumulation of ions near the ITO surface and (ii) the presence of CNTs in contact with the ITO-electrode. Those CNTs are polarized by the polarization of the electrodes and can themselves accumulate ions, leading to an enhanced capacitive phenomenon. (iii) Even in the presence of a continuous percolating network of CNTs between the electrodes, some "dead arms" are present. These "branches" do not allow the electrons to flow. Charges can then accumulate at those "dead arms", leading to a capacitive behavior of the CNTs-doped gels.

The structure of the gels has been observed with FE-SEM microscopy. The gels have been dried using supercritical CO_2, after exchanging the water content by ethanol. FE-SEM images are reported in Figure 3. These micrographs reveal the presence of well dispersed CNTs embedded in a silica matrix. This confirms the hypothesis of a CNTs network, dispersed homogeneously within the gel, that assures an electronic conduction. The silica network possesses a similar appearance in each sample. It is constituted of small silica beads agglomerated together, creating porosity at the mesoporous scale. Such a morphology is typical of the gels obtained by the condensation of sodium silicate in the presence of colloidal silica: the silicates polymerize with one another and around the colloids, aggregating the beads together.[35]

Cryogenic transmission electron micrography (cryo-TEM) allows to observe the system in a frozen state and to avoid the problems of reorganization of the sample upon drying. Figure 3F shows a cryo-TEM view of a suspension of CNTs and silica after ultrasonic dispersion. This indicates that the ultrasonic treatment is sufficient to disperse the CNTs, leading to isolated ones (or bundles constituted of a few entangled CNTs), without altering their length. The silica nanoparticles originating from the LUDOX HS-40 are left unmodified after this treatment.

Combining the different phenomena we identified to occur within the gel, we propose a model for the electrical properties of the system, whose equivalent electrical circuit is represented Figure 4. This electrical scheme can be decomposed in three parts, each one corresponding to an element of the system. A resistance R_e and an inductance L_e are placed upstream of the system to model the behavior of the ITO-electrodes. The migration of the ions is described by a resistor R_s associated in serial with a capacitive element Q_s. A constant phase element (CPE) ($Z = 1/Q(j\omega)^{\alpha}$) is used instead of a pure capacitor to take into account the nonideality of the electrodes. The part of the circuit corresponding to the presence of CNTs is placed in parallel with the ion migration branch. It is constituted of two branches in parallel: One is a pure resistance R_c to take into account the circulation of the electrons through the percolating network of CNTS. The other one is constituted of a capacity

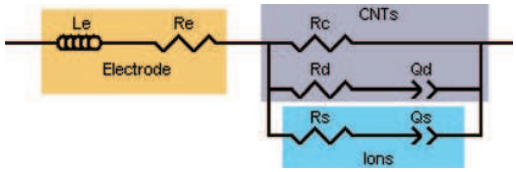

Figure 4. Equivalent electrical circuit used to model the behavior of the gel. L represents an inductance ($Z_L = jL\omega$), R a resistance ($Z_R = R$), and Q a constant phase element ($Z_Q = 1/Q(j\omega)^{\alpha}$). Under the percolation threshold, the R_c branch has to be removed to considerate the absence of a conductive network. Both the R_c and the R_d branches have to be removed to model GA-0 and GC-80.

Q_d and a resistance R_d to take into account the accumulation of charges at the surface of the CNTs in the "dead arms" of the network and the passage of the charges in the CNTs network before they reach the "dead arms". Once again, a CPE has been used to consider the nonideal character of the system. The R_c branch has to be removed from the sample that contains CNTs under the percolation threshold, as no continuous conduction pathway exists in this material. Similarly, both branches related to the presence of CNTs are removed to fit the impedance of samples that contains no CNTs. The experimental impedance diagrams have been fitted using EC-LAB v9.98[36] fitting functionalities.

The values of the parameters obtained with this model are reported in Table 1. Some graphical examples of the calculated data are presented in Figure 5. The fitted curves appear to be close to the experimental ones for the three types of sample (no CNTs, under and over the percolation threshold), supporting the validity of the model.

The resistance related to the migration of the ions in the wet gel, R_s, is in the same range for all types of samples (between 5 and 10 Ω) which is comparable to the value obtained for free ions in water. This is due to the fact that the gels have been synthesized using relatively dilute precursors, resulting in water occupying about 95% of the volume of the material. Hence, the migration of species within the gel is only slightly hindered by the solid phase, leading to similar values of R_s in the gel and in solution. In contrast, the value of Q_s and α_s, related to the interaction between the electrode and the ions, are very different between the samples that contains CNTs and the ones without. It can be explained by a modification of the surface of the ITO electrodes by CNTs. This coupling between the CNTs network and the ITO surface increases the dimension of the interface and hence increases Q_s. The presence of CNTs also increases the roughness of the electrode which becomes far from the ideal flat surface and has thus an associated α_s significantly different from 1.

For CNT-20 to CNT-80 ($c_{CNTs} > c_p$), the resistance of the conductive CNTs network, R_c, is in the same range as the resistance associated with the "dead arms" network, R_d. It corresponds to the fact that the conductive and the capacitive networks are expected to possess similar morphologies and thus comparable resistances. For the studied concentrations, R_d was comprised between 10^2 and 10^4 Ω. This value is quite different from the values of R_s (ca. 5−10 Ω for all the samples) and thus allows discriminating between the influence of the ion transport and the capacitive behavior of the CNTs network. The value of R_c logically decreases with the loading in CNTs, as more conductive materials is added in the sample. For CNT-20, CNT-40, and CNT-60, R_d was found to be lower with the loading, while Q_d increased, as more CNTs in the sample implies more "dead arms", having thus a larger capacity. R_d and Q_d were found to be respectively higher and lower in CNT-80 than in CNT-60. This can be explained by the increased viscosity of the sol that limits the dispersing effects of the ultrasounds and thus modifies the morphology of the network.

Evolution of the Gels. Figure 6 shows the evolution of the impedance diagrams for CNTs doped gels after several consecutive cycles. Gels that do not contain CNTs present no evolution over the different cycles of measurement, whereas gels that contain CNTs exhibit strong modifications in their response upon the different cycles. These modifications are mostly observable through the decrease of the diameter of the second semicircle in the Nyquist diagrams, which is related to the phenomena occurring in the CNT network. The responses of the materials after several cycles have been reported in Table A (Supporting Information).

The fitted values for the resistance of the ions in solution remain in the same range for all samples and over several cycles of measurement. This indicate that (i) the presence of CNTs in the system (in relatively low mass proportion) does not affect the migration of the ions in the liquid phase embedded in the gel and (ii) the structure of the silica network is not significantly perturbed during the repeated cycles. In the case of materials containing CNTs over the percolation threshold, the resistance of the conductive CNT network, R_c, decreases over several cycles. This decrease is very significant during the first cycles, but then R_c tends to stabilize. For instance, the

Table 1. Values of the Different Parameters Obtained after Fitting the Experimental Impedance Diagram with Our Model[a]

sample	GA-0	GC-80	CNT-10	CNT-15	CNT-20	CNT-40	CNT-60	CNT-80
L_e (μhartrees)	75 (1)	71 (1)	73 (1)	58 (1)	64 (1)	85 (1)	65 (1)	65 (1)
R_e (Ω)	98.4 (0.1)[c]	90.8 (0.1)[c]	84 (1)	64 (1)	70 (1)	95 (1)	75 (1)	75 (1)
R_c (Ω)	NA	NA	NA	NA	15900 (500)	853 (1)	397 (1)	220 (1)
R_d (Ω)	NA	NA	2870 (85)	3470 (6)	4030 (20)	641 (15)	189 (6)	210 (1)
$10^6 Q_d$[b]	NA	NA	15.4 (0.1)	398 (0.2)	854 (1)	1180 (10)	2830 (25)	2350 (40)
α_d	NA	NA	0.541	0.518	0.786	0.708	0.775	0.713
R_s (Ω)	NA	NA	5.1 (0.2)	4.3 (0.2)	4.4 (0.2)	8.5 (0.3)	5.8 (0.4)	6.1 (0.5)
$10^6 Q_s$[b]	19.8 (0.1)	18.1 (0.1)	23.0 (0.1)	126 (0.3)	212 (1)	110 (4)	181 (22)	119 (20)
α_d	0.975	0.976	0.953	0.739	0.686	0.802	0.7084	0.757
χ^2[d]	0.06402	0.0254	0.03624	0.05922	0.117	0.09076	0.02196	0.0107

[a]The values between parentheses represent the deviation of the fit, obtained with the simplex algorithm. [b]The unit of Q_x is F $s^{\alpha-1}$ and thus depends of α_x. [c]With our model, it is impossible to distinguish R_e from R_s for the sample that does not contain CNTs. The given values correspond to $R_e + R_s$. However, the value for R_s was found to be ca. 4Ω when using aluminum electrodes ($R_{eAl} \ll R_{eITO}$). [d]$\chi^2 = \sum_{i=1}^{n}(|Z_{Exp}(\omega_i) - Z_{Fit}(\omega_i)|^2)/(|Z_{Exp}(\omega_i)|^2)$.

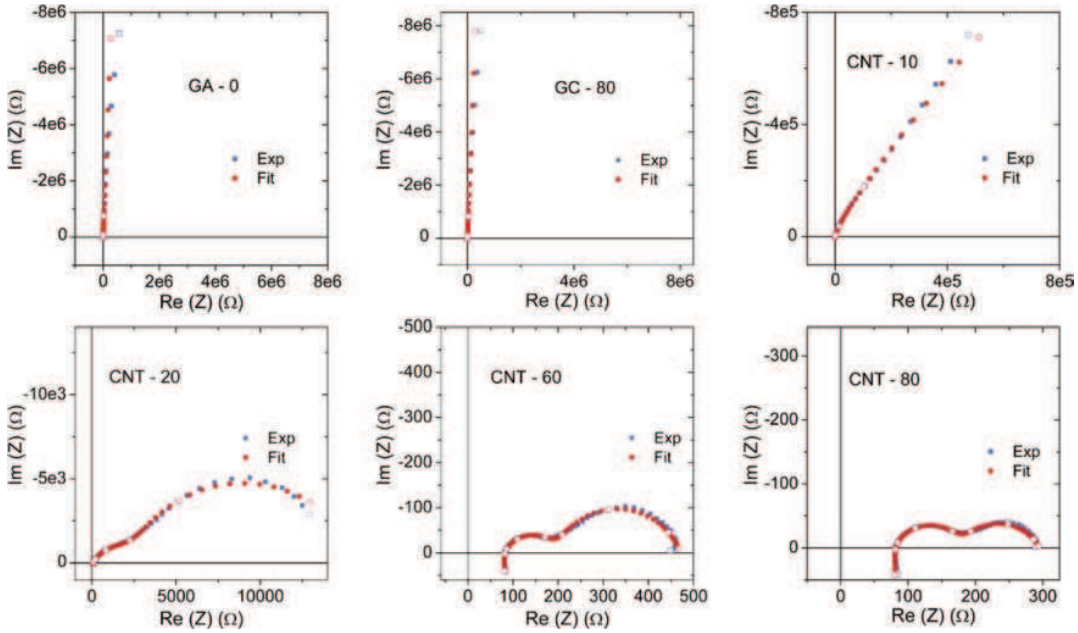

Figure 5. Measured and simulated Nyquist diagrams of CNT-doped gels (from left to right and up to down: GA-0, GC-80, CNT-10, CNT-20, CNT-60, CNT-80). The experimental values are represented with blue squares, and red circles are used for fitted values obtained with our model. The EIS experiments range from 100 kHz to 1 mHz (10 points/decade). Each open symbol represents a change of decade.

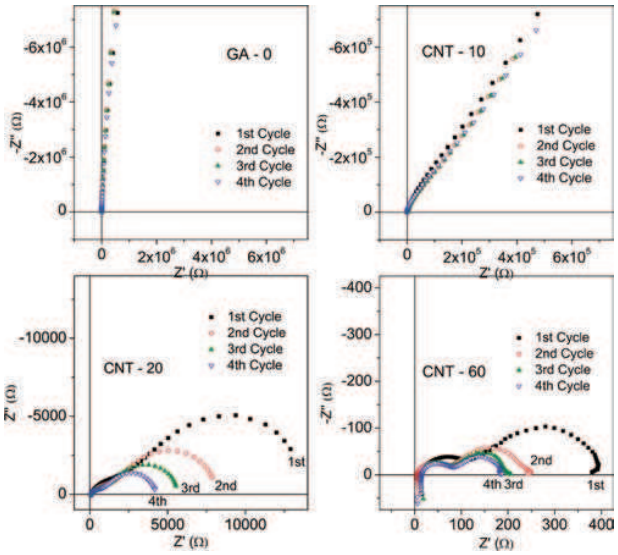

Figure 6. Nyquist diagrams recorded successively on GA-0 (top left), CNT-10 (top right), CNT-20 (bottom left), and CNT-60 (bottom right). The frequency ranges from 100 kHz to 1 mHz (10 points/decade).

calculated value of R_c for CNT-60 is equal to 396 Ω during the first cycle, but then stabilizes at 188 Ω after the fourth cycle.

We postulated that the decrease in resistance of the materials was related to a reorganization of the CNTs network. In solution, carbon nanotubes tend to align and form bundles that are stabilized by $\pi-\pi$ interactions between the tubes. This trend is the reason for the very poor dispersion of the CNTs in most usual solvents, rendering almost mandatory the use of a very strong stirring in presence of stabilizing agents (surfactants, polymers, etc.). Even if the CNTs are well-separated right after their dispersion, the lability of the solubilizing agents leads to a progressive reassociation of the tubes, resulting in the flocculation and then in the sedimentation of the suspension upon aging.[37] Our postulated model states that the tubes are initially well-dispersed in the gel material. This leads to only a few connections between the tubes, and thus results in a low conductivity, due to the lack of conduction pathways. During the evolution of the materials, the polymer wrapping around the nanotubes tends to be destabilized, resulting in an association of the CNTs. New conduction pathways within the gel are created, giving rise to an increase of its conductivity. It is also important to notice that the CNTs are at least partially immobilized within the silica matrix. If the partial immobilization allows the tube to connect together in local domain, it strongly hinders their mobility, preventing them to form massive bundles, which would then decrease the conductivity.

Figure 7 shows the evolution of the EIS answer after several consecutive measurements. The gel was aged 2 days before performing the measurements (measurements are about 5 min long). This difference in time scale allows us to consider that the clear difference between each impedance diagram is not only due to the natural aging of the gel, but rather to the application of a sinusoidal tension required to perform the EIS experiment. This effect was seen to occur even with small polarization of the sample (ΔE = 5 mV). For a given difference of potential, the resistance decreases and then stabilizes after several EIS cycles, but the application of a stronger polarization leads to a further decrease of the resistance. We postulate that the application of a difference of potential on a sample polarizes the CNTs. A negative polarization of the CNTs would destabilize the wrapping of carboxylate-bearing gum arabic and thus momentarily allows the CNTs to connect together. Electric fields have already been shown to induce an alignment of CNTs during the curing of polymer matrices.[38] However, the electric fields used in this former study are much higher (ca. 100 V/cm), and this alignment may be electrophoretic rather than driven by supramolecular interactions.

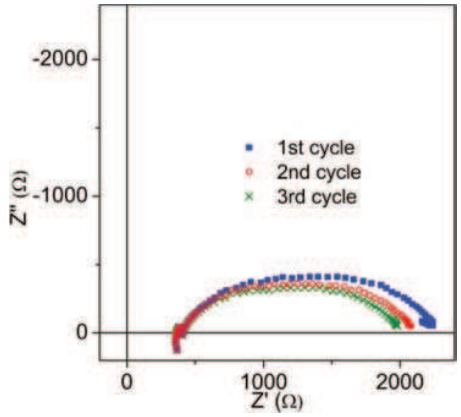

Figure 7. Succesive Nyquist diagrams recorded on CNT-60. The geometry of the sample has been modified by diminishing the size of the electrode, so that the contribution of the ions in solution is less marked. The measurements are done consecutively on a 2 days old gel. The frequency range from 100 kHz to 10 mHz (ΔE = 5 mV), and a measurement is about 5 min long. The clear evolution of an aged gel over this short period of time indicates that this evolution is induced by the measurement, instead of being time driven.

The conductivity of a conductive network over the percolation threshold follows a power law: $\sigma = \sigma_0(p - p_c)^m$, with p the volume fraction of conducting material and p_c the volume percolation fraction.[34] The former equation can be rewritten $\ln(\sigma_C) = \ln(\sigma_0) + m \ln(p - p_c)$. The value of the parameter p_c can be determined by adjusting its value so that all the $\ln(\sigma_C)$ are aligned on the log plot. Since p_c is dependent on the aspect ratio of the tubes (and thus on their length), which remains constant over the experiment, it can be postulated that the value of p_c is not modified during the evolution of the gel.

Adjusting the value of p_c to 0.175 ± 0.005 wt % causes the different sets of $\ln(\sigma_C)$ (measured after different numbers of EIS cycles) to be aligned (Figure 8). The value of m is given by the slope of the lines. m is equal to 1.37 ± 0.07 during the first cycle but decreases to 1.15 ± 0.06 after four cycles. m can be related to the dimensionality of the conductive network. The value of m for an ideal 3D connected network is equal to 2.0, 1.3 for a 2D network, and 1 for a 1D network.[34] It is noteworthy to add that this dimensionality refers to the conductive network and not to the geometry of the material. For instance, several unconnected ropes of nanotubes (1D objects) dispersed in a matrix (3D geometry) would still lead to a value of m equal to 1. The numerical values obtained for m after this adjustment indicate that the CNTs form a network were several tubes are aligned, instead of purely randomly dispersed. The further decrease of the value of m is coherent with a progressive alignment of the nanotubes within the matrix.

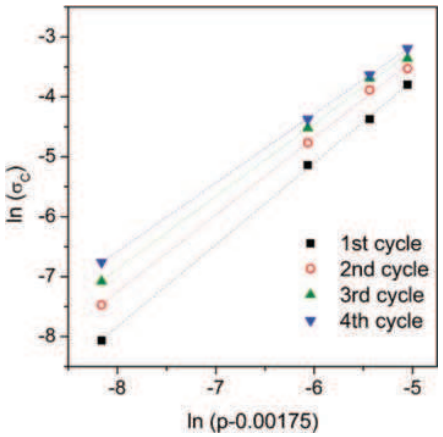

Figure 8. Plot of $\ln(\sigma_C)$ toward $\ln(p - 0.00175)$ over several consecutive EIS cycles. Since $\sigma = \sigma_0(p - p_c)^m$, m is given by the slope of the line and $\ln(\sigma_0)$ by the intersection with the ordinate axis. The parameters of the fits (dotted) by linear functions ($y = ax + b$) are: first cycle: a = 1.367 (0.020); b = 3.108 (0.127); R^2 = 0.999 35; second cycle: a = 1.286 (0.028); b = 3.034 (0.181); R^2 = 0.998 49; third cycle: a = 1.214 (0.028); b = 2.835 (0.179); R^2 = 0.998 35; fourth cycle: a = 1.147 (0.0042); b = 2.602 55 (0.027); R^2 = 0.999 96.

Raman spectroscopy has been used to study further the aggregation state of the nanotubes within the silica gels. This fast and nondestructive spectroscopy is particularly suitable for the study of CNTs, whose physical and chemical properties can be investigated through the presence of some very distinctive peaks.[39] Particularly, a study on DWCNTs realized by Puech et al.[40] has shown that the G band (ca. 1580 cm^{-1}) of bundled nanotubes is significantly broader than the one of isolated ones due to intertube couplings. In the present study, Raman spectroscopy has been used to determine the agglomeration state of the DWCNTS within the gel in order to establish a correlation with the increase in conductivity of the samples.

The study was focused on the behavior of CNT-60. This composition possesses a good electronic conductivity, and unlike CNT-80, the starting solution is not very viscous and can thus be easily processed. The gel was separated in three samples: CNT-60-0 was left unpolarized, CNT-60-25 was aged for 6 h under the application of the EIS sinusoidal polarization (DE = 25 mV), and CNT-60-150 was aged for 15 min under the application of a stronger polarization (DE = 150 mV). The observation of the G band (ca. 1580 cm^{-1}) of those samples is reported Figure 9. The G band appears to be composed of two overlapping Gaussian peaks corresponding to the vibrations of the inner and outer tubes.[40] The parameters of the peaks

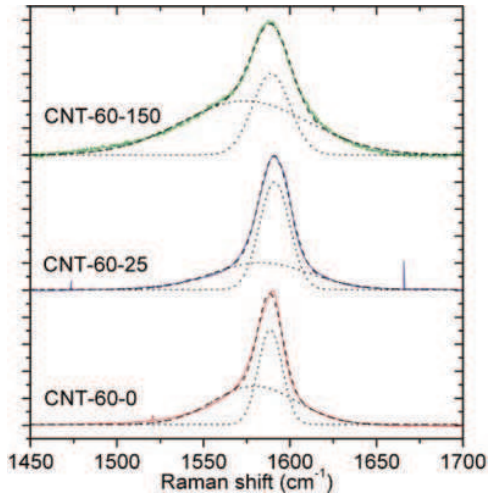

Figure 9. Raman spectra of the G band (ca. 1590 cm^{-1}) of CNT-60 samples. The gels have been left unpolarized (CNT-60-0), polarized by applying a sinusoidal 25 mV (CNT-60-25), and 150 mV (CNT-60-150) tension. Each peak is fitted as the sum (dash) of two Gaussian peaks (dot).

obtained after deconvolution are reported in Table 2. The full width at half-maximum (fwhm) of the outer tube vibration

Table 2. Parameters of the Gaussian Functions Used To Fit the DWCNTs G Band

		CNT-60-0	CNT-60-25	CNT-60-150
G band inner tube	fwhm (cm^{-1})	47	55	73
	ω (cm^{-1})	1579	1583	1573
G band outer tube	fwhm (cm^{-1})	14	17	21
	ω (cm^{-1})	1588	1591	1589

modes ranges from 14 cm^{-1} for the unpolarized sample to 21 cm^{-1} for the strongly polarized sample, while the fwhm of the inner tube vibration increases from 47 to 73 cm^{-1}. This broadening of both signals has been attributed to a bundling of the tubes upon polarization, thus corroborating the hypothesis of a reconnection of the CNTs network within the porous network of the gel. However, it must be added that a gel that have been aged over a relatively long time (1 week) before polarization did not show evolution both in its conductivity and in its Raman signal (data not shown). This could indicate that a certain mobility of the gel silica network is required to observe the rearrangement of the CNTs and that the ripening process naturally occurring within the gel could hinder the mobility of the nanotubes after a relatively long period of time.

4. CONCLUSION

Silica gels doped with DWCNTs were prepared using mild synthesis conditions. The CNTs network was found to percolate at 0.175 ± 0.005 wt %, and the conductivity reached 0.05 S/m for a 0.8 wt % doping rate. Wet gels exhibited both ionic and electronic conduction pathways, and a model was developed to determine quantitatively the parameters associated with those phenomena. The migration of the ions in the gel was shown to be mostly unaffected by the presence of the CNTs. An increase in conductivity occurred within the solidified gel upon several EIS analysis and was attributed to a reconnection of the CNTs network. This reconnection was shown to be at least partly electro-driven, and a sinusoidal polarization of 5 mV was sufficient to induce it. Raman spectroscopy confirms the aggregation of the CNTs. These data reveal unexpected evolution of the conductivity of CNT-doped gels, attributed to a reorganization of CNTs within soft hydrogels, a phenomenon that must be taken into account for the future design of electrochemical sensors based on CNTs-doped silica gels.

Corresponding Author
*E-mail: christel.laberty@upmc.fr.

ACKNOWLEDGMENTS

B.L.O. thanks Gervaise Mosser and Frédéric Herbst respectively for her and his help in performing the cryo-TEM and FE-SEM microscopies and gratefully acknowledges the Direction Générale de l'Armement (DGA) for its funding.

REFERENCES

(1) Popov, V. *Mater. Sci. Eng., R* **2004**, *43*, 61−102.
(2) Ruoff, R. *Carbon* **1995**, *33*, 925−930.
(3) Odom, T. W.; Huang, J. L.; Kim, P.; Lieber, C. M. *Nature* **1998**, *391*, 62−64.
(4) Yu, M. F.; Files, B.; Arepalli, S.; Ruoff, R. *Phys. Rev. Lett.* **2000**, *84*, 5552−5555.
(5) Berber, S.; Kwon, Y. K.; Tománek, D. *Phys. Rev. Lett.* **2000**, *84*, 4613−4616.
(6) Charlier, J. C.; Roche, S. *Rev. Mod. Phys.* **2007**, *79*, 677−732.
(7) Baughman, R. H.; Zakhidov, A. A.; de Heer, W. A. *Science* **2002**, *297*, 787−792.
(8) Schnorr, J. M.; Swager, T. M. *Chem. Mater.* **2011**, *23*, 646−657.
(9) Chou, T. W.; Gao, L.; Thostenson, E. T.; Zhang, Z.; Byun, J. H. *Compos. Sci. Technol.* **2010**, *70*, 1−19.
(10) Nishijima, H.; Kamo, S.; Akita, S.; Nakayama, Y.; Hohmura, K. I.; Yoshimura, S. H.; Takeyasu, K. *Appl. Phys. Lett.* **1999**, *74*, 4061−4063.
(11) Li, C.; Thostenson, E.; Chou, T. *Compos. Sci. Technol.* **2008**, *68*, 1227−1249.
(12) Aricò, A. S.; Bruce, P.; Scrosati, B.; Tarascon, J. M.; van Schalkwijk, W. *Nat. Mater.* **2005**, *4*, 366−377.
(13) Avouris, P. *Acc. Chem. Res.* **2002**, *35*, 1026−1034.
(14) de Heer, W. A.; Châtelain, A.; Ugarte, D. *Science* **1995**, *270*, 1179−1180.
(15) Li, J.; Ma, P. C.; Chow, W. S.; To, C. K.; Tang, B. Z.; Kim, J. K. *Adv. Funct. Mater.* **2007**, *17*, 3207−3215.
(16) Sandler, J.; Shaffer, M. S. P.; Prasse, T.; Bauhofer, W.; Schulte, K.; Windle, A. H. *Polymer* **1999**, *40*, 5967−5971.
(17) Thostenson, E. T.; Ren, Z.; Chou, T. W. *Compos. Sci. Technol.* **2001**, *61*, 1899−1912.
(18) Rul, S.; Lefèvre-Schlick, F.; Capria, E.; Laurent, C.; Peigney, A. *Acta Mater.* **2004**, *52*, 1061−1067.
(19) Ajayan, P. M.; Stephan, O.; Colliex, C.; Trauth, D. *Science* **1994**, *265*, 1212−1214.
(20) Moniruzzaman, M.; Winey, K. I. *Macromolecules* **2006**, *39*, 5194−5205.
(21) Flahaut, E.; Peigney, A.; Laurent, C.; Marlière, C.; Chastel, F.; Rousset, A. *Acta Mater.* **2000**, *48*, 3803−3812.
(22) Cho, J.; Boccaccini, A. R.; Shaffer, M. S. P. *J. Mater. Sci.* **2009**, *44*, 1934−1951.
(23) Gavalas, V. G.; Andrews, R.; Bhattacharyya, D.; Bachas, L. G. *Nano Lett.* **2001**, *1*, 719−721.
(24) Jung de Andrade, M.; Lima, M. D.; Stein, L.; Pérez, C.; Roth, S. *Phys. Status Solidi B* **2007**, *244*, 4218−4222.
(25) Zhang, L. M.; Wang, G. H.; Xing, Z. *J. Mater. Chem.* **2011**, *21*, 4650−4656.
(26) Zhu, L.; Tian, C.; Zhai, J.; Yang, R. *Sens. Actuators, B* **2007**, *125*, 254−261.
(27) Gavalas, V. G.; Law, S. A.; Ball, J. C.; Andrews, R.; Bachas, L. G. *Anal. Biochem.* **2004**, *329*, 247−252.
(28) Brinker, C. J.; Scherer, G. W. *Sol-Gel Science: The Physics and Chemistry of Sol-Gel Processing*; Academic Press: Boston, 1990.
(29) Lima, M. D.; Andrade, M. J.; Skákalová, V.; Bergmann, C. P.; Roth, S. *J. Mater. Chem.* **2007**, *17*, 4846−4853.
(30) Bandyopadhyaya, R.; Nativ-Roth, E.; Regev, O.; Yerushalmi-Rozen, R. *Nano Lett.* **2002**, *2*, 25−28.
(31) Mouchet, F.; Landois, P.; Datsyuk, V.; Puech, P.; Pinelli, E.; Flahaut, E.; Gauthier, L. *Environ. Toxicol.* **2011**, *26*, 136−145.
(32) Flahaut, E.; Bacsa, R.; Peigney, A.; Laurent, C. *Chem. Commun.* **2003**, 1442−1443.

(33) Osman, M. E.; Menzies, A. R.; Williams, P. A.; Phillips, G. O.; Baldwin, T. C. *Carbohyd. Res.* **1993**, *246*, 303−318.
(34) Stauffer, D., Aharony, A. *Introduction to Percolation Theory*, Rev. 2nd ed.; Taylor & Francis: London, 1994.
(35) Nassif, N.; Bouvet, O. M. M.; Rager, M. N.; Roux, C.; Coradin, T.; Livage, J. *Nat. Mater.* **2002**, *1*, 42−44.
(36) EC-Lab, Bio-Logic - Science Instruments, 2009.
(37) Shaffer, M. S. P.; Fan, X.; Windle, A. H. *Carbon* **1998**, *36*, 1603−1612.
(38) Martin, C. A.; Sandler, J. K. W.; Windle, A. H.; Schwarz, M. K.; Bauhofer, W.; Schulte, K.; Shaffer, M. S. P. *Polymer* **2005**, *46*, 877−886.
(39) Dresselhaus, M. S.; Dresselhaus, G.; Jorio, A. *Annu. Rev. Mater. Res.* **2004**, *34*, 247−278.
(40) Puech, P.; Nanot, S.; Raquet, B.; Broto, J. M.; Millot, M.; Anwar, A. W.; Flahaut, E.; Bacsa, W. *Phys. Status Solidi B* **2011**, *248*, 974−979.